

Online Detection of Straight Lines in 3-D Ultrasound Image Volumes for Image-Guided Needle Navigation

Heinrich Martin Overhoff, Stefan Bußmann

University of Applied Sciences Gelsenkirchen, Gelsenkirchen, Germany
heinrich-martin.overhoff@fh-gelsenkirchen.de

Abstract. 3D ultrasound imaging can be a valuable tool in navigated interventions. When used as continuous imaging device, it can not only show the anatomical site but has the potential to measure instrument positions, e.g. to validate the data of position localizer tools. Real time image analysis is a prerequisite for this concept. Needle-like instruments can be idealized by lines. An algorithm was implemented in C that determines four parameters of an equation of a line in 3D space from voxel positions. It mainly consists of a sequence of two 2-D Hough transforms, which determine the instrument's orientation and location. The execution time of the algorithm's C implementation was measured on a PC platform for varying numbers of instrument and error-prone voxels. For a moderate number of voxels, real time demands for the 4DoF position determination can be fulfilled.

1 Introduction

Planar (2-D) sonography is a well established online imaging modality to visualize anatomical structures during interventions like biopsies or punctures. Typically, a needle guiding device is fixed to the ultrasound transducer and aligned to the ultrasound image plane. The needle is oriented oblique to the image plane and therefore only partially visible in the sonograms. To navigate the needle during an intervention, image plane, anatomical structures and landmarks (e.g. vessels) must be properly aligned.

Interstitial high dose rate brachytherapy is a local radiooncologic therapy where radioactive sources are temporarily placed in catheters, that are themselves inserted using needle-like devices, so-called applicators [1]. Pre-interventional ultrasound imaging is increasingly used to detect and delineate organs and tumors for isodose planning in brachytherapy. Usually, the applicator placement is done "blind", without online imaging, but this can potentially be overcome using intra-interventional spatial (3D) ultrasound imaging. Reflections of anatomical structures like connective tissue or muscles can interfere with the applicator's reflections. Thus, adapting only the opacity transfer function when visualizing such an ultrasound image volume might neither be sufficient for the visualization nor for measuring the applicator's position.

For determining the location, orientation and tip (5 degrees of freedom (DoF)) of a needle-like instrument relative to an ultrasound image volume [2], an electromagnetic position measurement system is an option. In a clinical setup with 3D ultrasound imaging, an image based instrument pose determination can be of interest to validate location and orientation measurements (4 DoF). Such image volumes are analyzed by a new algorithm which was implemented in common C. The running time of that C program on standard hardware is measured to evaluate if real time demands are fulfilled.

2 Materials and Methods

Image volumes were acquired with a BC431E motorized 3D curved array transducer attached to a MyLab70 ultrasound device (Esaote Europe B.V., Maastricht, The Netherlands). An image volume consisted of approximately 250 images of 420×480 gray-scale pixels. For continuous acquisition, an acquisition rate of $r = 0.25$ volumes/second was assumed, resulting in a data rate of r volumes/second \cdot 250 images/volume \cdot $420 \cdot 480$ pixels/image \cdot 8 bit/pixel \approx 384.5 Mbit/second. Assuming additional processing times, e.g. for data transfer, image pre-processing, visualization and operating system activities, an execution time per volume $T_{\text{exec}} \leq 1$ second $\ll \frac{1}{r}$ was determined to fulfill real time demands.

For determining the applicator's pose, it is assumed that the applicator does not bend during the interactive feed motion. Thus, it is possible to presume that the reflections of the needle are represented by straight lines in all image volumes. The number of needle reflections or needle points \mathbf{r} respectively and the number of additional noise points varies in ultrasound image volumes, e.g. due to variable imaging properties or the needle length recorded in the image volume.

Such needle points \mathbf{r} fulfill the vector form of the equation of a line

$$\mathbf{r} - \mathbf{r}_0 - \lambda \mathbf{u} = \mathbf{0} \quad (1)$$

where \mathbf{u} denotes the direction and \mathbf{r}_0 the origin point vector. For an identical line, there is an infinite number of such representations. The equation of a line becomes unique, if the two conditions

$$\mathbf{u}^T \cdot \mathbf{u} = 1 \quad (2)$$

$$\mathbf{u}^T \cdot \mathbf{r}_0 = 0 \quad (3)$$

are fulfilled, i.e. if the length of the direction vector \mathbf{u} is normalized and origin point vector \mathbf{r}_0 and direction vector \mathbf{u} are perpendicular. Under these conditions, the equation of a line (Eq. 1) can be transformed into the pair of equations

$$\mathbf{u} \times (\mathbf{r} - \mathbf{r}_0 - \lambda \mathbf{u}) = \mathbf{u} \times (\mathbf{r} - \mathbf{r}_0) = \mathbf{0} \quad (4)$$

$$\mathbf{u}^T \cdot (\mathbf{r} - \mathbf{r}_0 - \lambda \mathbf{u}) = \mathbf{u}^T \cdot \mathbf{r} - \lambda = 0 \quad (5)$$

It contains five parameters: two components u_x and u_y of the direction vector \mathbf{u} , two components r_{0x} and r_{0y} of the origin point vector \mathbf{r}_0 which together define the line as a whole, and λ , which defines an individual point on the line.

A sequence of two 2-D Hough transforms was chosen to reduce the complexity compared to a 4-D Hough transform [3, 4]. The following algorithm was implemented to determine the four line parameters u_x , u_y and r_{0x} , r_{0y} for N_r scattered, noisy line voxels and additional N_{noise} noise voxels:

1. Direct binarization of the image volume to get N voxels $\mathbf{r}_i, 1 \leq i \leq N$, $N = N_r + N_{\text{noise}}$ being candidates for applicator reflections.
2. 2-D Hough transform for the \mathbf{u} -components: $\mathbf{u} \times (\mathbf{r}_i - \mathbf{r}_0) - \mathbf{u} \times (\mathbf{r}_j - \mathbf{r}_0) = \mathbf{u} \times (\mathbf{r}_i - \mathbf{r}_j) = -(\mathbf{r}_i - \mathbf{r}_j) \times \mathbf{u} = \mathbf{0}$, $1 \leq i \leq N - 1, i < j \leq N$ and (Eq. 2) determine \mathbf{u}

$$-(\mathbf{r}_i - \mathbf{r}_j) \times \mathbf{u} = \begin{bmatrix} 0 & r_{iz} - r_{jz} & r_{jy} - r_{iy} \\ r_{jz} - r_{iz} & 0 & r_{ix} - r_{jx} \\ r_{iy} - r_{jy} & r_{jx} - r_{ix} & 0 \end{bmatrix} \cdot \mathbf{u} = \mathbf{R}_{ij} \cdot \mathbf{u} = \mathbf{0} \quad (6)$$

Since $\text{rank}(\mathbf{R}_{ij}) = 2$, e.g. the third line of the system (Eq. 6) is substituted by (Eq. 2) to make it uniquely solvable. This leads to a non-linear equation system. If $u_z < 0$, $\mathbf{u} = -\mathbf{u}$. Component pair (u_x, u_y) is incremented.

3. Select the component pair (u_x^*, u_y^*) with maximal number of increments and calculate the optimal direction vector \mathbf{u}^* with (Eq. 2) for $u_z \geq 0$.
4. 2-D Hough transform for the \mathbf{r}_0 -components: With (Eq. 4) and $\mathbf{u} = \mathbf{u}^*$, the linear equation system for \mathbf{r}_0 follows

$$\mathbf{u} \times \mathbf{r}_0 = \begin{bmatrix} 0 & -u_z & u_y \\ u_z & 0 & -u_x \\ -u_y & u_x & 0 \end{bmatrix} \cdot \mathbf{r}_0 = \mathbf{U} \cdot \mathbf{r}_0 = \mathbf{u} \times \mathbf{r}_i = \mathbf{b}_i = \begin{bmatrix} b_1 \\ b_2 \\ b_3 \end{bmatrix} \quad (7)$$

Since $\text{rank}(\mathbf{U}) = 2$, e.g. the third line of the system (Eq. 7) is substituted by (Eq. 3) to make it uniquely solvable, where the component pair (r_{0x}, r_{0y}) is incremented.

$$\begin{bmatrix} 0 & -u_z & u_y \\ u_z & 0 & -u_x \\ u_x & u_y & u_z \end{bmatrix} \cdot \mathbf{r}_0 = \begin{bmatrix} b_1 \\ b_2 \\ 0 \end{bmatrix} \quad (8)$$

5. Select the component pair (r_{0x}^*, r_{0y}^*) with maximal number of increments and calculate optimal direction vector \mathbf{r}_0^* with (Eq. 3).

Parallel needles have identical direction vectors \mathbf{u} . Parallel lines are discriminable, if \mathbf{r}_0 is noted in a rotated coordinate system where the z -axis is parallel to \mathbf{u} . In this case, different parallel needles have different (r_{0x}, r_{0y}) -pairs due to (Eq. 3), and the number of cluster points is equal to the number of needles.

3 Results

For a PC equipped with an Intel Core2Duo E8400 3 GHz processor and 3 GB RAM, the main board FSB frequency was 1333 MHz, and the C code was compiled on Windows XP Professional using Visual Studio 2008 with the SSE 2 instruction-set enabled. The processing times of the resulting program were measured for different numbers N of voxels \mathbf{r} for a resolution of $\Delta u_x = \Delta u_y = 0.01$. As table Tab. 1 shows, the running time is mainly determined by calculation of \mathbf{u} in comparison with the calculation of \mathbf{r}_0 . For less than approximately 5000 voxels, the real time demand $T_{\text{exec}} < 1$ second is fulfilled.

Figure 1 shows two exemplary synthetic data sets. In 1000 test cases, the difference angles between at random defined and determined direction vectors \mathbf{u} were less than 10° (median 3°), and the difference vectors between defined and determined origin point vector \mathbf{r}_0 had euclidean distances less than 0.6 (median 0.5).

4 Discussion

With the implemented algorithm, the real time demand $T_{\text{exec}} < 1$ second for the estimation of the 4 DoF position of a needle-like instrument can be fulfilled for up to 5000 scattered voxels detected in an ultrasound image volume.

Ongoing work is dedicated towards further minimization of the execution time T_{exec} , e.g. by a multithreading implementation of the algorithm and the detection of noise voxels.

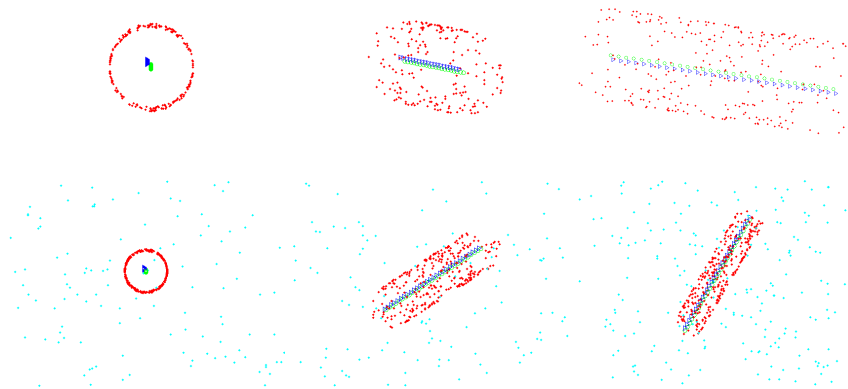


Fig. 1. Lines detected for synthetic tubes of length $L = 100$ and radius $R = 10$ with $N = 1000$ points. Upper row: Tube (red dots) with symmetry axis (green circles) and axis detected by the algorithm (blue triangles). View from above (left column) and two oblique views (center and right columns). Bottom row: the same as the upper row with additional noise data.

Table 1. Execution times.

Number of Points	Total Execution Time	Time for \mathbf{u}	Time for \mathbf{r}_0
N	$T_{\text{exec}}/\text{seconds}$	$T_{\mathbf{u}}/\text{seconds}$	$T_{\mathbf{r}_0}/\text{seconds}$
1000	0.117	0.116	0.000135
2000	0.238	0.238	0.000275
3000	0.431	0.431	0.000377
4000	0.679	0.679	0.000530
5000	1.021	1.020	0.000619
6000	1.380	1.375	0.000823
7000	1.816	1.808	0.000895
8000	2.325	2.311	0.001006
9000	2.844	2.842	0.001190
10000	3.541	3.539	0.001304

References

1. Brenner DJ. Radiation biology in brachytherapy. *J Surg Oncol.* 1997;65.
2. Hartmann P, Baumhauer M, Rassweiler J, et al. Automatic needle segmentation in 3D ultrasound data using a hough transform approach. In: *Proc BVM*; 2009. p. 341–5.
3. Hough P, inventor; P.V.C., assignee. Method and Means for Recognizing Complex Patterns, U.S.patent 3069654. U.S.patent 3069654, 1962; 1962.
4. Illingworth J, Kittler J. A survey of the hough transform. *Computer Vis Graph Image Process.* 1988;44:87–116.